JOURNAL OF MATERIALS SCIENCE 24 (1989) 1941–1945

HREM study of atomic image of single crystal indium phosphide

WANG LU CHUN, FENG DUAN, TAN KE MIN, CHEN JUN, YIAN YONG
Department of Physics and Institute of Solid State Physics, Nanjing University, Nanjing, 210008, People's Republic of China

This paper reports some experimental results of high resolution electron microscopy (HREM) studies on single crystal indium phosphide (InP) along the [0 0 1] zone axis. Using 400 kV electrons, with defocus value about 46.0 nm, the optimum conditions for structure imaging for both In and P atoms were found to be about 26.0 nm. Decreasing the specimen thickness to about 15.0 nm, only atomic images of P remain; increasing the specimen thickness to about 37.0 nm, only atomic images of In remain. These experimental results are in good agreement with computer simulation. It was also observed that for bent crystal deviating from the [0 0 1] axis, the bright spots, corresponding to In and P atomic columns in high resolution structure imaging, are elongated at a deviation angle equal to 0.18 degrees, the two bright spots are connected together along the direction of the [1 1 0] zone axis. This phenomenon is also confirmed by computer simulation. In the experiment, a pair of dislocation waves were observed with apparent Burgers vectors of $\frac{1}{2}[0\,1\,0]$ and $\frac{1}{2}[0\,\bar{1}\,0]$ while the actual Burgers vectors may be $\frac{1}{2}[0\,1\,1]$ and $\frac{1}{2}[0\,\bar{1}\,\bar{1}]$.

1. Introduction

Indium phosphide is a compound semiconductor [1, 2] which is widely used in microwave and optoelectronic devices [3]. The microstructure and defects in this material are very important for understanding their potential influence on the device properties. Brown [4], Mahajan [5], Muller [6], have reported their observations of defects by means of TEM techniques. In this paper some preliminary HREM studies on this material are reported.

It should be noted that with the rapid development of HREM techniques and theoretical studies, Hashimoto [7], Crewe [8], Bourr [9] and their colleagues have reported many significant facts in direct observation of structural or atomic images. However, few reports are presented about imaging both heavy and light atoms simultaneously along certain zone axis. Here we demonstrate that both heavy indium and light phosphide atoms can be imaged simultaneously under certain conditions. The computer simulation is in good agreement with the experimental results.

2. Experimental results

The InP single crystal was grown by liquid encapsulation Czochralski (LEC) method. The specimens for electron microscope observation were prepared by crushing technique. The observation were performed on Jeol-400EX electron microscope (Cs = 1 mm, Cc = 1.7 mm) at 400 kV.

Indium phosphide has a cubic zinc sulphide structure with the space group $F\bar{4}3m$. The structure may be viewed as two interpenetrating face centred cubic (f c c) lattices, occupied by In and P respectively, which are displaced from each other by one-quarter of a body diagonal. The unit cell parameter is a = 0.5868 nm. The structure model is shown schematically in Fig. 1, in which In atoms are located on the $\frac{1}{4}$ and $\frac{3}{4}$ position. Fig. 2 is a two-dimensional projection along [0 0 1] zone axis of the structure, in which open circles represent P atoms, while the black ones represent In atoms. Each indium atom in the pattern, has four neighbouring P atoms and vice versa. Fig. 3 shows a high resolution structure image along [0 0 1] zone axis. The defocus value of objective lenses is Δf = 46.0 nm, which is very close to the scherzer condition. ($\Delta f = \lambda^{1/2}\mathrm{Cc}^{1/2}$ about $\Delta f = -40.6$ nm.) The inset on the upper left corner of Fig. 3 is the selected-area electron diffraction patterns of InP along [0 0 1] direction. The inset on the right side of Fig. 3 is the image of computer simulation with specimen thickness about 25.5 nm. The computer simulation was carried out with the multislice method based on dynamical theory of electron diffraction and image formation, the thickness of slice was chosen to be H = 0.5868 nm, just equal to that of a unit cell. In the high resolution structure

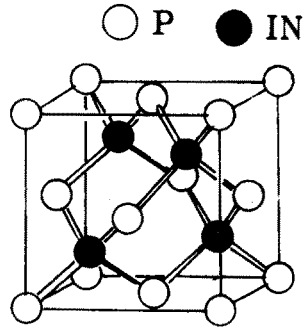

Figure 1 Structure model for InP.

0022–2461/89 $03.00 + .12

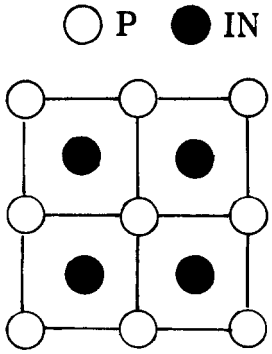

Figure 2 The projection of P and In atoms of InP along [0 0 1] axis.

image, every two bright spots 0.207 nm apart constitute the two-dimensional image which is consistent with those shown in Fig. 2 and computed image. Thus the one-to-one relationship is established between bright spots and projected atomic columns. The influence of specimen thickness on the formation of image is displayed in Fig. 4. The observed image varies in the picture as the specimen of thickness increases from left to right. The inset on the left side of the picture is the image of computer simulation with thickness of $H = 15.0$ nm, and the inset in the middle part is that of thickness of $H = 25.5$ nm, while the inset on the right side is that thickness of $H = 37.0$ nm.

The calculated image coincides well with the observed image. In the middle part (the thickness of specimen is about 25.5 nm), the structure image containing both light P atoms and heavy In atoms is clearly shown; on the left side, only atomic images corresponding to light P atoms are shown; while on the right side, only atomic images corresponding to heavy In atoms, thus structure image are observed. In the transition region, the contrasts of the phosphide spots and indium spots vary with specimen thickness gradually. Fig. 5 shows an HREM image of bent crystal. As shown in Fig. 6 when the incident electron

TABLE I Structure factor of InP

hkl	F	F
200	−12.14	−25.14
220	28.51	19.00
400	19.74	14.06
420	−7.69	−12.69

F the structure factors of InP.
F the structure factors taking only heavy atoms of InP into account.

beam deviates from the [0 0 1] zone axis, the two bright spots of representing In atoms and P atoms will be elongate along [1 1 0] direction, until the two bright spots are connected together. The process is clearly shown in Fig. 7 and supported by computer simulation with deviation angle equal to 0.18° rotated along [1 1 0] shown in the inset on the right corner in Fig. 5.

Fig. 10 is a lattice image along [0 0 1] zone axis and shows a pair of dislocations with the edge components $\frac{1}{2}[0\,1\,0]$, $\frac{1}{2}[0\,\bar{1}\,0]$. Since effect of the screw components of the dislocation is missing in HREM image, actually these may be a pair of dislocations with Burgers vectors $\frac{1}{2}[0\,1\,1]$ and $\frac{1}{2}[0\,\bar{1}\,\bar{1}]$, which is the dislocation with shortest lattice vectors in f c c lattice. The $\vec{b}_1 = \frac{1}{2}[0\,1\,0]$ is represented symbolically by $\top$ and $\vec{b}_2 = \frac{1}{2}[0\,\bar{1}\,0]$ represented by $\perp$. Here the dislocations in pairs were appeared in the local micro-distortion region. Fig. 11 shows a pair of dislocations with the edge components $\frac{1}{2}[0\,1\,0]$ and $\frac{1}{2}[0\,\bar{1}\,0]$ of a structure model in InP. Due to the distortion of crystal structure, the contrast of bright spots of atomic columns projection was evidently different from the perfect structure in Fig. 10.

3. Discussion

It should be noted that our results cannot be explained well enough with weak-phase object approximation. Because the specimen thickness exceeds the requirement for weak-phase object approximation, that is

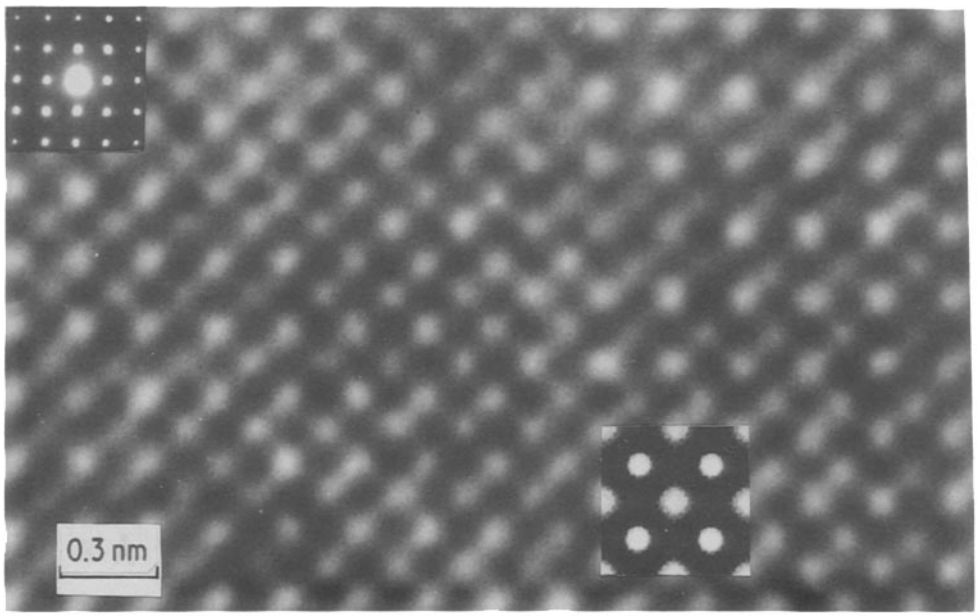

Figure 3 A structure image of InP in [0 0 1] zone axis. The inset in the left upper corner is electron diffraction pattern of In [0 0 1] orientation. The inset on the right side is the image of computer simulation. Spherical aberration coefficient Cc = 1 mm; specimen thickness $H = 26.0$ nm; objective lens defocus $F = -46.0$ nm.

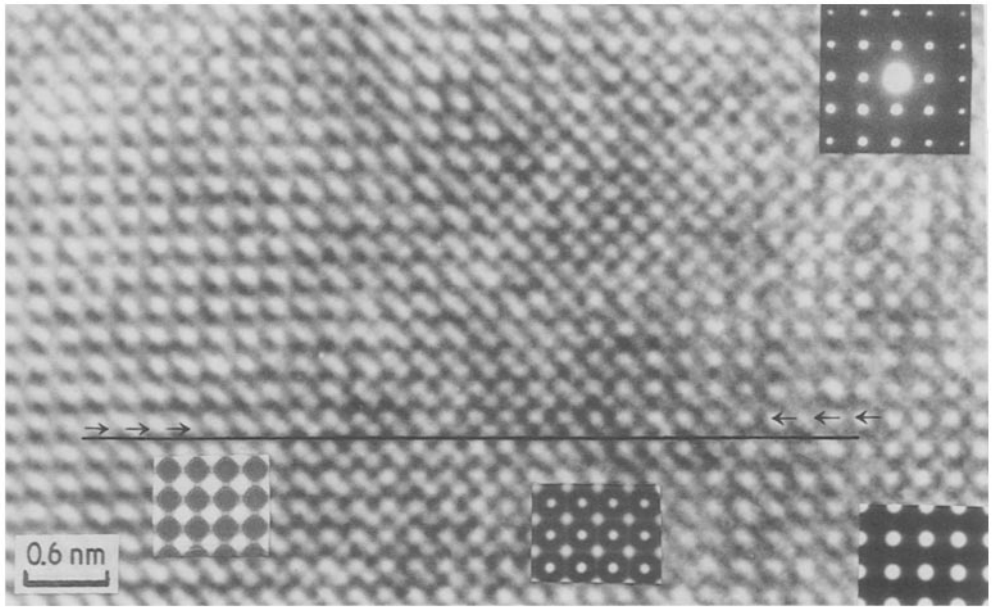

Figure 4 The variation of structure image against specimen thickness is shown in this figure. The insets below the black bar are images of computer simulation, defocus $F = -46.0$ nm, left side $H = 15.0$ nm, in the middle $H = 25.5$ nm, right side $H = 37.0$ nm. The inset in the upper right corner is the diffraction pattern.

$\mathscr{Z}\phi(X \cdot Y) \ll 1$, here $\mathscr{Z} = \pi/\lambda v$ is the interaction constant and $\phi(X \cdot Y)$ is the projected potential function of the specimen along Z direction [10]. For InP, the unit cell parameter $a = 0.5868$ nm, the thickness should be less than 2.5 nm if weak-phase object approximation is satisfied. The experimental results show the optimum thickness condition for structure image of InP is about 26.0 nm. Only computer simulation based on dynamical diffraction theory can explain the experimental results satisfactorily.

It is well known that different atoms have different scattering factors. In InP the scattering factor of heavy In atom is about twice or threefold that of light P atom, (in the range $\sin\theta/\lambda = 0 \sim 2$) shown in Fig. 8. Table I gives the ordinary structure factors F of InP and the structure factor F' which is calculated by only considering the heavy atoms. Comparison of F and F' shows that the structure factors of 2 2 0 and 4 0 0 do not change much. This indicates that the amplitudes of diffracted waves of (2 2 0) and (4 0 0) are mainly contributed by the heavy In atoms. While the structure factors of 2 0 0 and 4 2 0 change a lot, this indicates that the amplitudes of diffracted waves of (2 0 0) and (4 2 0) are contributed mainly by the light P atoms [10].

The amplitudes from various lattice planes of InP crystal in the [0 0 1] zone axis for various thicknesses were calculated by using the dynamical theory of electron diffraction. Fig. 9 shows the thickness dependence of the amplitudes for several main diffracted waves. The calculated images at the different thickness indicated by the arrows a, b, c, are also shown in these figures. It can be seen that with increasing specimen thickness, the amplitudes of diffracted waves of 2 0 0 and 4 2 0 oscillate with a period of about 20.0 nm and for the 2 2 0 and 4 0 0 waves oscillate with a period of about 10.0 nm, while the amplitudes of transmitted beam with a period of about 40.0 nm were oscillated. When the amplitude of transmitted waves is near its

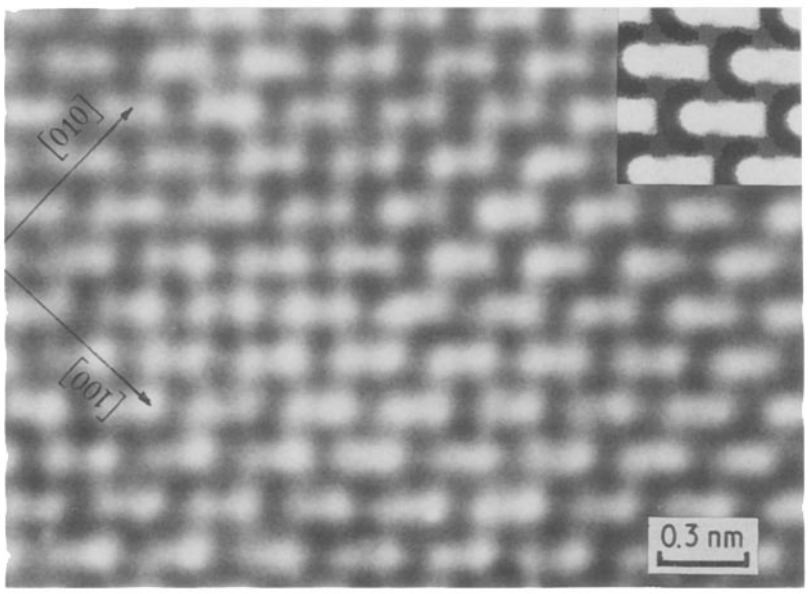

Figure 5 High resolution image for bent crystal. The inset in the upper right corner is the image of computer simulation (specimen thickness $H = 26.0$ nm). The incident electron beam tilted at 0.18° angle with the [0 0 1] zone axis.

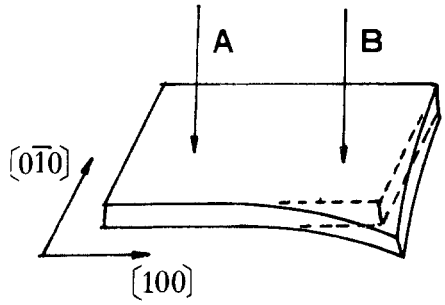

Figure 6 The schematic diagram for bent crystal. The incident beams are labelled by A, B.

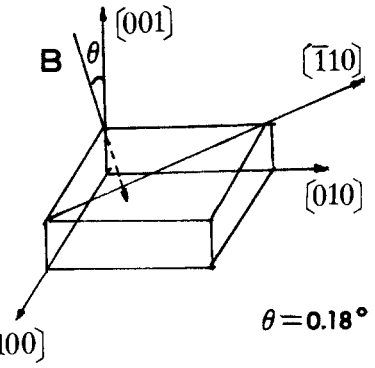

Figure 7 The schematic diagram for the inclined incident beam and the crystal. The orientation of incident beam rotates about 0.18° at [1 1 0] zone axis.

minimal value, atomic image will be obtained. It is indicated, thus the transmitted beam interacts with diffracted beams according to the dynamical theory of electron diffraction, so that when the amplitude of transmitted beam approximates to that of diffracted beam, both P and In atomic columns may be imaged (at b); when the amplitudes of the 2 0 0 wave stronger than the 2 2 0 and 4 0 0 waves, only the bright spots

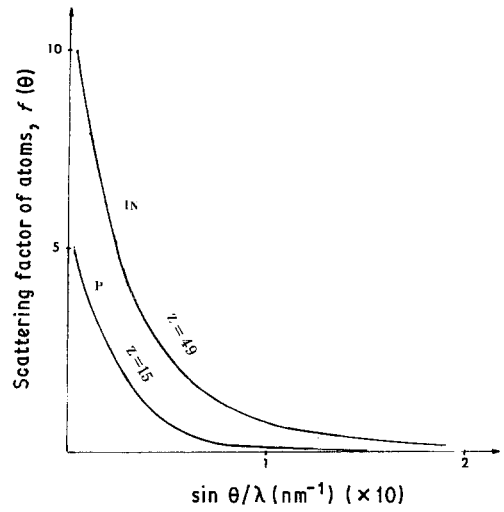

Figure 8 The scattering factors for P and In atoms against sin θ/λ.

representing P atomic columns are imaged (at a); when the amplitudes of the 2 2 0 wave are stronger than the 2 0 0 and 4 2 0 waves, only the bright spots representing In atomic columns are imaged (at c). On the other hand, the variation of amplitudes of transmitted and diffracted beam against specimen thickness may be seen in Fig. 9. From a to b and from b to c, the thickness of specimen changes about 10.0 nm. The above analysis indicates, that due to dynamical effect of interaction between transmitted beam and diffracted beams, while the amplitude of transmitted wave is near its minimum, high-resolution structure image showing both kinds of atomic images will be formed, but when the amplitude of transmission wave becomes stronger than diffracted waves, only structure image showing one kind of atomic images will be formed [11].

The local micro-distortion discovered in experiment

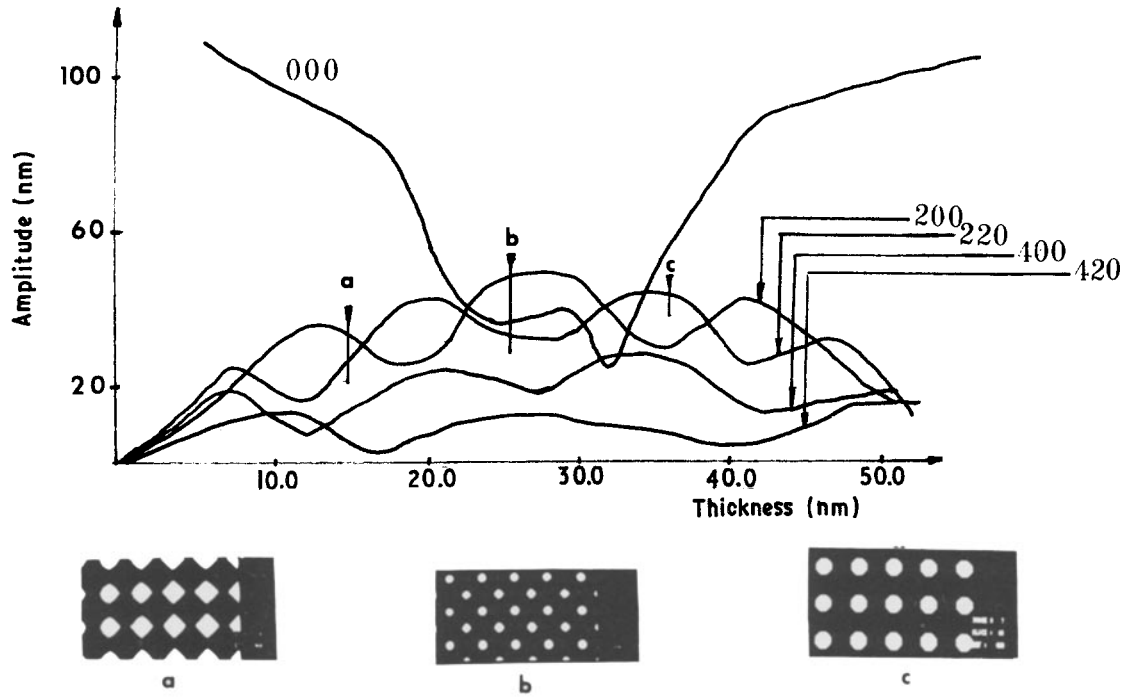

Figure 9 The amplitudes of the 0 0 0, 2 0 0, 2 2 0, 4 0 0, 4 2 0, waves against specimen thickness in InP. The images simulated at the thicknesses 15.0, 25.5 and 37.0 nm, respectively.

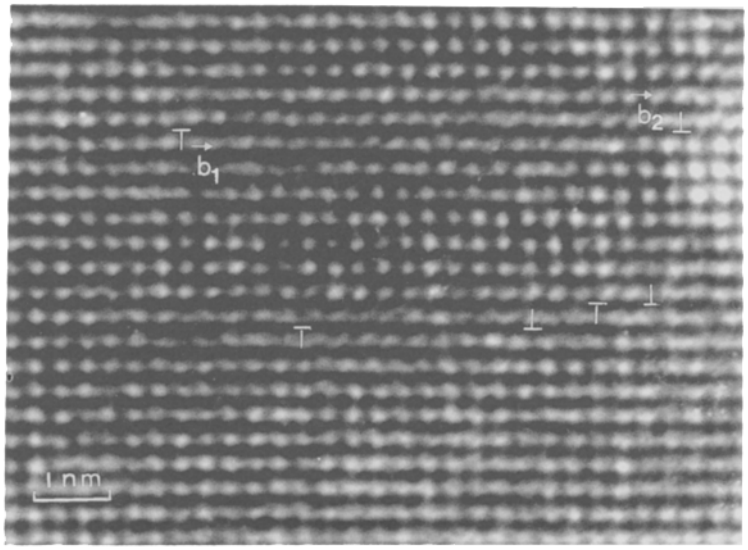

Figure 10 A lattice image of InP along [0 0 1] axis, the dislocation with apparent Burgers vectors $\vec{b_1} = \frac{1}{2}[0\,1\,0]$ and $\vec{b_2} = \frac{1}{2}[0\,\bar{1}\,0]$ is shown in this figure.

is probably produced in the process of crystal growth with non-uniform thermal stress fields. Since In–P bond energy is relatively small, the micro-distortion is easily formed in the region of higher stress [12, 13]. Thus the crystal lattices seriously distorts on the slip plane of the dislocation and its neighbour. Because the dislocations of opposite sign were the metastable state, will lead to attract each other to reduce their total elastic energy until they combine and annihilate each other.

It is one of the reasons that the defects in crystals may be induced by the local micro-distortion, this may be important to the semiconductor.

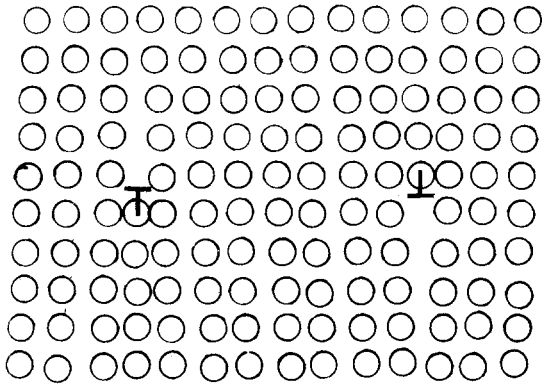

Figure 11 The schematic diagram for a pair of dislocations with the edge components $\frac{1}{2}[0\,1\,0]$, $\frac{1}{2}[0\,\bar{1}\,0]$.

Acknowledgements

Thanks are due to Professor Li Qi for his help in the work. The authors are also grateful for Professor Chu I Ming for providing computer program for the multi-slice calculation on microcomputer.

References

1. A. G. FOYT, *J. Cryst. Grow.* **54** (1981) 1.
2. B. COCKAYNE, *ibid.* **54** (1981) 9.
3. "Information of Semiconductor" (Beijing, 1986) 10.
4. G. T. BROWN, B. COCKAYNE and W. R. MACEWAN, *J. Elec. Mater.* **12** (1983) 93.
5. S. MAHAJAN and A. K. CHIN, *J. Cryst. Growth* **54** (1985) 138.
6. G. MÜLLER, R. RUPP, J. VÖLKL, H. WOLF and W. BLUM, *J. Cryst. Growth* **71** (1985) 771.
7. H. HASHIMOTO, H. ENDOH, T. TANJI, A. ONO and M. WATONBE, *J. Phys. Soc. Jpn* **42** (1977) 1073.
8. A. V. CREWE, *Chemica Scripta* **14** (1978–1979) 17.
9. A. BOURRET and J.-M. PENISSON, *JEOL News* **1** (1987) 1.
9. K. H. KUO and H. Q. YE, "High Resolution Electron Microscopy" (Science Press, Beijing, 1985).
10. R. GUAN, H. HASHMOTO and T. YOSHIDA, *Acta. Cryst.* **B40** (1984) 109.
11. R. GUAN, H. HASHMOTO and K. H. KUO, *Ultramicroscopy* **20** (1986) 195.
12. A. S. JORDON, *J. Cryst. Grow.* **70** (1984) 555.
13. Y. SEKI, *J. Appl. Phys.* **49** (1978) 822.

Received 17 May
and accepted 12 September 1988